[9] H. S. Hewitt, "A computer designed 720 to 1 microwave compression filter," *IEEE Trans. Microwave Theory Tech.*, vol. MTT-15, pp. 687–694, Dec. 1967.
[10] R. Sato "A design method for meander-line networks using equivalent circuit transformations," *IEEE Trans. Microwave Theory Tech.*, vol. MTT-19, pp. 431–442, May 1971.
[11] P. I. Richards, "Resistor transmission-line circuits," *Proc. IRE*, vol. 36, pp. 217–220, Feb. 1948.
[12] J. W. Bandler, "Optimization methods for computer-aided design," *IEEE Trans. Microwave Theory Tech.*, vol. MTT-17, pp. 533–552, Aug. 1969.
[13] W. J. Getsinger, "Coupled rectangular bars between parallel plates," *IRE Trans. Microwave Theory Tech.*, vol. MTT-10, pp. 65–73, Jan. 1962.
[14] R. J. Wenzel, "Small elliptic-function low-pass filters and other applications of microwave *C* sections," *IEEE Trans. Microwave Theory Tech.*, vol. MTT-18, pp. 1150–1158, Dec. 1970.
[15] G. I. Zysman and A. Matsumoto, "Properties of microwave *C*-sections," *IEEE Trans. Circuit Theory*, vol. CT-12, pp. 74–82, Mar. 1965.

Efficient Capacitance Calculations for Three-Dimensional Multiconductor Systems

ALBERT E. RUEHLI AND PIERCE A. BRENNAN

Abstract—**The design and packaging of integrated circuits requires the calculation of capacitances for three-dimensional conductors located on parallel planes. An integral-equation (IE) computer-solution technique is presented, which provides accurate results. The solution technique minimizes computer storage requirements while maintaining calculating efficiency without excessive computation times.**

I. Introduction

IN THE PAST, integral-equation (IE) techniques found extensive use in capacitance calculations for two-dimensional geometries [1]–[7]. These solutions have proven to be very useful for systems involving sets of long parallel transmission lines (conductors) in a multidielectric environment. Further, for sufficiently high frequencies and TEM-mode propagation, the characteristic impedance can be found [8]. Thus all electrical parameters required for a complete characterization of a set of low-loss transmission lines are obtainable from the IE approach.

Three-dimensional capacitance calculations, however, have been limited to small problems. The capacitance of an infinitely thin square plate has been considered by several authors [9]–[13], while the capacitance between parallel plates [14] and for a cube has been found [15]. Recently, solutions have been obtained for problems involving infinite dielectric regions [16]–[18] by using Green's function techniques similar to those used in the two-dimensional calculations cited above.

The numerical solution of the IE leads to a matrix that resembles the coefficients of potential for multiconductors. In a two-dimensional analysis, the unknowns represent the surface charge (on the boundary of a cross section), and are therefore one dimensional. Approximately 30 unknowns lead to a good solution for an average problem on a small computer since the matrix requires only 900 words of storage.

Manuscript received May 30, 1972; revised July 28, 1972.
The authors are with the IBM Thomas J. Watson Research Center, Yorktown Heights, N. Y. 10598.

In contrast to this, the unknowns representing the surface charge will be two dimensional when the IE approach is applied to a three-dimensional capacitance problem. If the above example is extended to this case, matrices larger than 1000×1000 result, requiring excessive storage for a direct matrix inversion. This presents a serious limitation to three-dimensional calculations especially since the matrices are full. The solutions introduced here considerably reduce storage requirements for the matrix of coefficients without unduly increasing computation complexity, allowing the treatment of three-dimensional conductors on multiple planes.

In some situations, the presence of closely spaced ground planes makes a two-dimensional description [1]–[7] possible, and thus a transmission-line characterization suffices. However, if ground planes are remote or not present, three-dimensional solutions become necessary. Specifically, the use of partial capacitances (defined later) in conjunction with partial inductances [19] leads to a three-dimensional technique, and partial-element equivalent circuits [20] result in a complete characterization of three-dimensional interconnection structures.

In Section II, the formulation of the IE solution is developed, while Section III is devoted to the numerical solution. In Section IV, the evaluation of the coefficient matrix is considered, and in Section V, Green's functions for the inclusion of infinite interfaces are considered. Important relations to multicapacitance concepts are established in Section VI, while comparisons with other results are made in Section VII.

II. Integral-Equation Formulation

A set of K conductors is considered with or without infinite ground planes or with infinite dielectric regions present. The potential $\Phi(\bar{r}_i)$ at a field point $\bar{r}_i$ in the system is

$$\Phi(\bar{r}_i) = \sum_{k=1}^{K} \int_{s_k} G(\bar{r}_i, \bar{r}') q(\bar{r}')\, ds' \qquad (1)$$

where q is the charge density on the conductor surfaces s_k and

G is the appropriate Green's function for the infinite interfaces present. For a uniform infinite dielectric region surrounding the conductors, $G = G_D$ where

$$G_D = \frac{1}{4\pi\epsilon} \frac{1}{|\bar{r}_i - \bar{r}'|} \tag{2}$$

ϵ is the permittivity, and $\bar{r}'$ is the vector from the origin to the source point. In this paper, all results are obtained with $1/4\pi\epsilon_0 = 0.0089876$ pF/m, with ϵ_0 being the permittivity of air. Equations (1) and (2) represent a system of Fredholm equations of the first kind with an integrable singular kernel G.

For simplicity, the surfaces of the conductors are assumed to conform with the Cartesian coordinates and all conductor surfaces s_k are divided into a set of N_k contiguous cells of area S_k. Therefore,

$$\sum_{k=1}^{K} \int_{s_k} = \sum_{k=1}^{K} \sum_{j=1}^{N_k} \int_{S_j}.$$

Use is made of the mean value theorem [21] to remove the charge density from under the integral sign:

$$\int_{S_j} G(\bar{r}_i, \bar{r}') q(\bar{r}')\, ds' = q(\bar{\xi}_j) \int_{S} G(\bar{r}_i, \bar{r}')\, ds'. \tag{3}$$

The vector $\bar{\xi}_j$ is located somewhere on the jth cell and $q(\bar{\xi}_j)$ is bounded by the smallest and largest value of the charge density on the cell except for the conductor edge, where q is infinite. Equation (1) is rewritten using (3) as

$$\Phi(\bar{r}_i) = \sum_{k=1}^{K} \sum_{j=1}^{N_k} q(\bar{\xi}_j) \int_{S} G(\bar{r}_i, \bar{r}')\, ds'. \tag{4}$$

For the usual subarea method or collocation solution (e.g., [10]), the potential vector is matched to the known potential at the center of all cells in the system and $q(\bar{\xi}_j)$ is assumed to be of constant density over cell j. Thus both potential and charge density are approximated in the collocation approach.

If, however, (4) is integrated over cell i and $q(\bar{\xi}_j)$ is assumed to be a constant cell density, a solution by Galerkin's method results [22]. The left-hand side is then $\Phi_i S_i$ since all cells are equipotential surfaces, where Φ_i is the cell potential and S_i is its area. Hence, for the new solution, (4) is replaced by

$$\Phi_i = \sum_{k=1}^{K} \sum_{j=1}^{N_k} q(\bar{\xi}_j) \frac{1}{S_i} \int_{S_i} \int_{S_j} G(\bar{r}, \bar{r}')\, ds' ds \tag{5}$$

for $i = 1, 2, \cdots, N_T$, where N_T is the total number of cells in the system. The solution pursued here corresponds to a variational solution [12], [23].

III. Solution for Charges

In the collocation solution, the matrix system formed by (4) (matched at the center of all N_T cells) is inverted to obtain the charge density. Similarly, the charges are found for the new solution using (5). The approximation of $q(\bar{\xi}_j)$ by a constant charge density, rather than being represented by the mean value equation (3), is particularly poor near the sharp convex corners of the conductors due to the steep slope of the charge density surface caused by the singularity. Cells decreasing in size towards the corners have been used before to obtain more accurate capacitance values (e.g., [2]). This represents an improvement in the constant value approximation of (3).

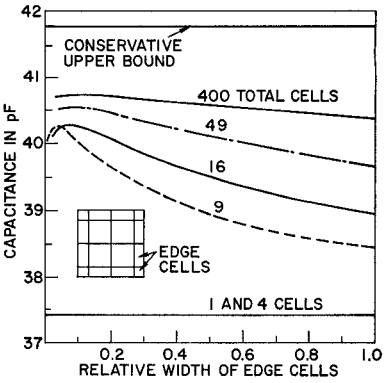

Fig. 1. Capacitance of square plate as function of relative edge cell size.

The system matrix corresponding to both discrete systems [(4), (5)] will become ill-conditioned for a large number of cells N_T due to the singularity in the charge density. This problem is even worse if the cell size is decreased towards the corners. In [13] a new solution is suggested to eliminate this problem but, as is apparent from Fig. 4, the solution accuracy is not improved by this technique. As an alternate approach [24], the conditioning of the system matrix is improved by solving for the average total charge on the cells $Q_{sj} = S_j q(\bar{\xi}_j)$, rather than the density, and by decreasing the cell size towards the corner. For example, for a circular disk [25], the singularity at the edge is of the form $d^{-1/2}$, where d is a small distance from the edge. After integration, the total charge on the edge cell Q is proportional to $d^{1/2}$, which is zero in the limit as $d \to 0$. If the edge cells are chosen to be smaller than the center cells, the large elements of the charge density vector $q(\bar{\xi}_j)$ are compensated for by a small area S_j so that a more uniform total charge vector is obtained. For example, in [3] it is shown that, at least for a circular disk, a sinusoidal cell distribution leads to constant total charge on all cells. The system of equations (5) is rewritten in terms of total charge as

$$\Phi_i = \sum_{k=1}^{K} \sum_{j=1}^{N_k} ps_{ij} Qs_j \tag{6a}$$

where

$$ps_{ij} \triangleq \frac{1}{S_i S_j} \int_{S_i} \int_{S_j} G(\bar{r}, \bar{r}')\, ds' ds \tag{6b}$$

for $i = 1, 2, \cdots, N_T$. Equation (6)[1] forms a system of symmetric algebraic equations that is solved for the charges Qs_j.

It is proposed that for the three-dimensional solutions only one cell along the sharp corners be decreased in width, since the total number of cells per conductor must necessarily be few. Further, for closely spaced conductors, the coupling capacitance depends on the center cell charge as well as the corner distribution, and thus the center of the conductor surfaces cannot be depleted of cells. An edge cell of 0.1 times the width of the uniform center cells leads to accurate results for both the infinitely thin plate and the cube. This is illustrated in Fig. 1 for the infinitely thin plate. The upper-bound solution [26] in Fig. 1 is conservative for the thin plate. It is

[1] It was pointed out by a reviewer that this expression coincides with Sylvester's potential averaging approximation [7].

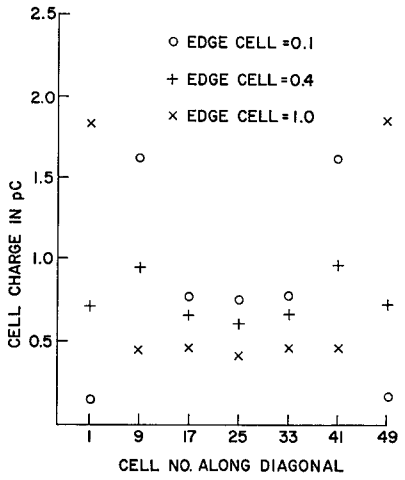

Fig. 2. Cell charges with respect to edge cell size for plate.

noted that the Galerkin solution satisfies the conditions of Thomson's theorem [8], and thus the solutions obtained represent lower bounds on the capactiance [2].

It has been stated above that the conditioning of the system matrix is improved by solving (6) for the total charges with a decrease in the edge cell size. The magnitude of the total charge on the cells along the diagonal is shown in Fig. 2 for a thin plate with seven cells per side. The most uniform cell charge is obtained with an edge cell of 0.4, while the best capacitance is obtained for an edge cell of 0.1 Fig. (1). A good criterion for the conditioning of a matrix is given by the condition number [27] as cond $(A)=|\lambda(A)|$ max/$|\lambda(A)|$ min, where $\lambda(A)$ represents an eigenvalue of the matrix A. In some of the experiments given, the condition number was monitored and found to be small; thus the corresponding matrices are well conditioned. For the case in Fig. 2 and an edge cell size of less than 0.4, an increase is found, as expected. For example, for the thin plate with seven cells per side, cond $(ps)=21$ for an edge cell of 0.4, while for 0.1, cond $(ps)=30$. It is easy to see that both the capacitance improvement and the conditioning improvement by the edge cells has a maximum, since the total charge on very narrow edge cells is insignificantly small with a small contribution to the capacitance.

IV. Coefficient Matrix

It is noted by inspection of (6b) that the coefficient matrix for the new solution is symmetric. Further, (6a) can be written in matrix form as

$$\Phi s = ps\,Qs \tag{7}$$

where Φs is the vector of cell potentials and Qs represents the total cell charge. The ps-matrix can be viewed as the matrix of coefficients of potential for the subdivided system. The inverse of the ps-matrix $ps^{-1} \triangleq cs$ is most efficiently computed by Choleski's method [28], which also requires the least amount of storage [only $0.5N_T(N_T+1)$ words]. It is shown that the ps-matrix is positive definite, as required for Choleski's method. The energy needed to assemble the charges in the system, corresponding to (7), is positive independent of the particular choice of the nonzero charges Q. However, the energy can be written as a quadratic form $W_e=0.5Q^T ps\,Q$, which proves that ps is a positive definite matrix.

A closed-form answer can be found for the coefficients of

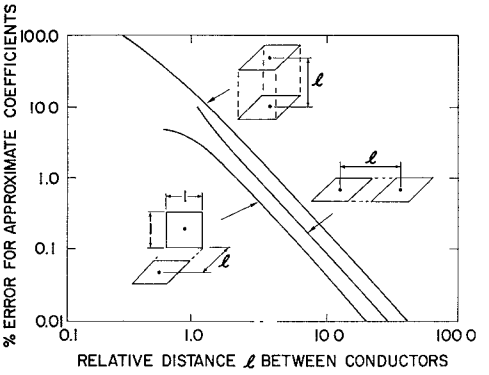

Fig. 3. Relative error due to point approximation.

the ps-matrix with minor changes from a formulation for inductance calculations [29], which provides coefficients for both parallel and perpendicular cells. The coefficients are given in the Appendix in a general form such that all relative locations are considered. Evaluation of the coefficients in subroutine form takes an average of 2 ms on an IBM 360/91 computer programmed in double-precision Fortran. A point source law given by G_D [(2)] is used to approximate both coefficients [(15), (16)]. A comparison between the exact coefficients and G_D is given in Fig. 3 for all relative locations of importance, where the relative error E is defined as

$$E = \frac{100\,|\,ps_{ii} - G_D\,|}{ps_{ij}}\,. \tag{8}$$

A relative distance R between the cell centers of $R>2$ for the use of the approximation $ps_{ij}=G_D$ suffices for many cases, since only a few cells in any given geometry will be located at exactly this distance. The computation of G_D takes only 50 μs on an IBM 360/91 computer, including the decision tests. Thus the gain in computation time is about 40. The time to compute the ps-matrix will especially be reduced for multibody problems and for problems with a large number of small cells, since the condition $R>2$ is satisfied for most of the cells.

It is interesting to note some properties of the ps-matrix. For a K conductor system, K square submatrices along the diagonal correspond to the cells on the conductors themselves, while all off-diagonal submatrices correspond to conductor-to-conductor coupling. Conductors can be added or deleted by simply adding or deleting the appropriate submatrices to the ps-matrix, without recomputation of the entire matrix. The matrices resulting from the IE method are full and little sparsity can be gained by setting small elements to zero. In fact, systems with small nonimportant intercoupling should be partitioned into a set of smaller problems wherever possible.

V. Green's Functions

Different dielectric regions and ground planes are included in the formulation by appropriate Green's functions. It is not the purpose of the present paper to give a complete list of Green's functions, since many results already are available in the literature [5]–[7], [16], [17] for a multitude of cases. Three-dimensional Green's functions are obtained from the same set of images as the corresponding two-dimensional cases. Since most of the Green's functions can be found from

image solutions, they are generalized as

$$G = \sum_n \alpha_n G_{D_n} \tag{9}$$

where α_n is an appropriate constant coefficient and G_{D_n} indicates the location of the nth image. For a single dielectric or conducting interface, the summation has only two terms, and thus the time required to compute the ps_n-matrix will increase by less than a factor of two. An interesting result is obtained for very thin conductors located on a dielectric half space with permittivity ϵ_a. Since the images coincide almost with the conductors, the dielectric is taken into account by a new dielectric constant $\epsilon_{av}=0.5(\epsilon_0+\epsilon_a)$. Thus the dielectric is easily included in the free-space solution without increasing the computation time.

If, for geometries requiring infinitely many images, G given by (9) converges uniformly, integration and summation can be interchanged in (6b). Then, the new elements of the ps-matrix are given by

$$ps_{ij}{}^I = \sum_n \alpha_n (ps_{ij})_n \tag{10}$$

where again the subscript n indicates the appropriate location for the image coefficient ps_{ij}. For practical calculations, only a small number of terms is included in the series. The convergence of the series depends strongly on the grouping of the terms. Kittel [30] gives a general rule for the improvement of convergence for the calculation of the Madelung constant by grouping the terms into electrically neutral entities. This technique is applied to the case where conductors are bounded by two conducting planes, since convergence is slower for this case than for dielectric interfaces where the image strength decreases with increasing z. If groups of four images are formed, the coefficients are

$$ps_{ij}{}^I = \frac{1}{4\pi\epsilon}\sum_{n=1}^{N}\{(ps_{ij})_{[z_i-z_j-2(n-1)H]} - (ps_{ij})_{[z_i+z_j+2(n-1)H]} + (ps_{ij})_{[z_i-z_j+2nH]} - (ps_{ij})_{[z_i+z_j-2nH]}\} \tag{11}$$

where N is the number of image quadrupoles included. One of the infinite ground planes is located at $z=0$, while the second ground plane is at $z=H$.

The distance of the nth image quadrupole from $z=0$ is approximately $|z|=2nH$, which increases rapidly with n. Thus approximate coefficients can be used for distant images. The approximate error term e_r for the truncated series is found by integration over the remainder of the series analogous to the integral test for convergence. A closed form for e_r is found for $(ps_{ij})_n = G_{D_n}$ as

$$4\pi\epsilon e_r = \frac{1}{2H}\ln\frac{[A_2+(A_2{}^2+u^2)^{1/2}][A_4+(A_4{}^2+u^2)^{1/2}]}{[A_1+(A_1{}^2+u^2)^{1/2}][A_3+(A_3{}^2+u^2)^{1/2}]}. \tag{12a}$$

Here, the following definitions are used:

$$\begin{aligned} u^2 &= (x_i - x_j)^2 + (y_i - y_j)^2 \\ A_1 &= |z_i - z_j - 2(N-\tfrac{1}{2})H| \\ A_2 &= |z_i + z_j + 2(N-\tfrac{1}{2})H| \\ A_3 &= |z_i - z_j + 2(N+\tfrac{1}{2})H| \\ A_4 &= |z_i + z_j - 2(N+\tfrac{1}{2})H|. \end{aligned} \tag{12b}$$

The error e_r can be used as a criterion to find the maximum number of terms in the series of (11). A more convenient heuristic formula can be obtained suitable for an *a priori* estimate of N. If the contribution of the remaining terms is to be small, $2NH$ must be larger than u in (12b). Thus the number of terms in the series is estimated by $N=K_1+K_2u/H \leq N_{\max}$. All constants depend on the range of problems and the desired solution accuracy. The number of terms N is limited by $N_{\max}$ to save computation time for long conductors between closely spaced planes, since the coefficients $ps_{ij}{}^I$ are extremely small for cells spaced by a large u. In all computations conducted, all coefficients are improved by adding e_r to $ps_{ij}{}^I$. An example for the application of this scheme and for the constants is given in Section VII. Again, for the situation of multiple dielectric interfaces, less terms must be included in the series, since the strength of the nth image α_n decreases with increasing $z=2nH$.

VI. Relation to Multicapacitances

All the different capacitance matrices of interest are available from the coefficients of capacitance [31], which are obtained from the subcoefficients after solution of (7) as

$$\boldsymbol{Q}s = cs\boldsymbol{\Phi}s \tag{13}$$

where $cs=ps^{-1}$ is called the matrix of subcoefficients of capacitance. The coefficients of capacitance matrix $\boldsymbol{c}$ are easily found from

$$c_{lm} = \sum_{l=1}^{NT}\sum_{m=1}^{NT} cs_{lm}1_l 1_m \tag{14}$$

where, in general, $1_l=1_m=1$ for cells on conductors l and m, respectively, and $1_l=1_m=0$ for cells not on the respective conductors.

Next, the coefficients of partial capacitance matrix cp are considered. They represent coefficients in an environment where the conductor surfaces are partitioned into an appropriate set of "partial" conductor surfaces that can assume different potentials. Again, they find use in high-frequency equivalent circuit models [20]. Coefficients of partial capacitance are given by [(14)] except $1_l=1_m=1$ for the cell on the jth and mth *partial* surface only. Both the capacitance matrix C and, equivalently, the matrix of partial capacitances C_p are found by well-known relations [31].

VII. Results and Comparison

It is first noted that all answers given below can be scaled for different dimensional units by multiplication of the C-matrix by the linear conversion factor to meters. Such a conversion is desirable in a computer program, since small dimensional numbers that can cause roundoff errors are avoided.

An infinitely thin square plate is the nontrivial three-dimensional capacitance problem considered most often, and it therefore serves as a yardstick for a comparison of solution methods. In Fig. 4 all solutions known to the authors are compared. The first solution due to Maxwell [9] of 40.13 pF was obtained by using the symmetry of the structure and modified corner coefficients such that the results could be computed for six cells per side without a computer. Collocation solutions have been obtained by many authors [10]–[14]. Here, the collocation solution is extended to 30 cells by using physical symmetry; the capacitance for this case is 40.35 pF. For the

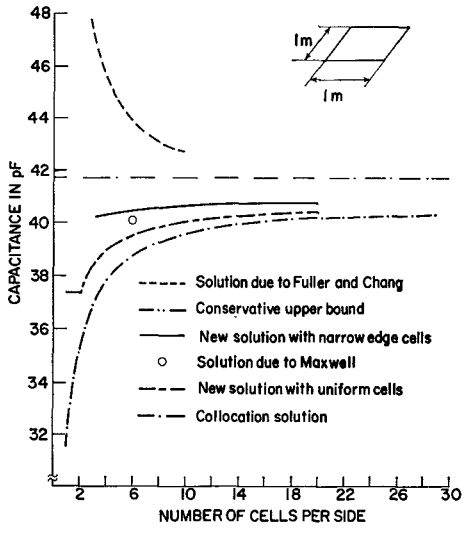

Fig. 4. Capacitance of thin square plate versus cells per side.

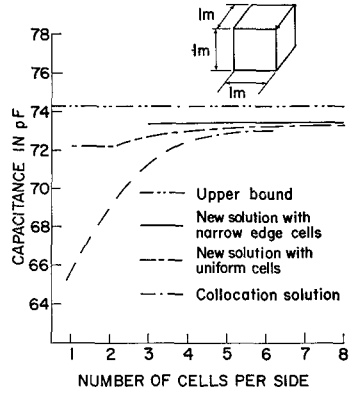

Fig. 5. Capacitance of cube versus cells per side.

Galerkin solution presented here, 40.38 pF is obtained with only 20 uniform cells per side. Further, a substantial improvement is obtained if the nonuniform edge scheme is implemented. The capacitance for this case is 40.54 pF for only seven cells per side with an edge cell of 0.1. Use is not made of the physical symmetry in the new results given, since the complex structures to which this formulation addresses itself do not necessarily possess such symmetries. However, the symmetric matrices are solved by Choleski's method (Section IV).

The upper- and lower-bound solutions for the cube (Fig. 5) are almost a factor of two better than those obtained for the square plate in Fig. 4. It is noted that for this case, the new solution with nonuniform edge cells is only a weak function of the number of cells indicating convergence. Also, the capacitance obtained with eight uniform cells per side (73.27 pF) is less than that of the answer for three cells per side with an edge cell of 0.1 (73.35 pF). For a cube with three cells per side, the computation time on an IBM 360/91 computer is 2.5 s for setting up the matrix coefficients and 0.14 s for matrix inversion, where $R>2$ is used for the approximate coefficients. For six cells per side, the matrix is set up in 20 s while matrix inversion takes 7.6 s. It can easily be shown that no improvement in capacitance is gained by increasing the cells per side from one to two in the Galerkin solution. This is indicated in both Figs. 4 and 5. Comparisons with the two-dimensional solutions are made to show the effect of a finite length on capacitance. Three transmission lines above a common ground plane shown in Table I are considered (where all distances are in millimeters). All sides are divided into three cells in this solution. Table I shows a comparison between the new solution and the two-dimensional solution due to Weeks [6]. For the shorter line length (length/width = 10), the three-dimensional solution clearly shows the differences in the coefficients of capacitance per unit length.

A problem considered by Kammler [3] with a known answer for an infinite length is used as an illustration for the two-ground plane solution. The structure consists of an infinitely thin conductor of width 0.6 m centered between two plates spaced at 1 m with an exact capacitance of 368.1 pF. In the three-dimensional solution, the center conductor of a length of 10 m is divided into three cells along the width and six cells along its length. A capacitance of 373.7 pF is obtained with the formulation for the Green's function of Section V, where specifically $K_1=6$, $K_2=10$, and $N_{\max}=50$. For this solution the relative distance chosen for the approximate coefficients in Fig. 3 is $R>30$, since an increased accuracy is required for the almost equal coefficients in (11).

The use of the solution presented is greatly facilitated for generalized computations if the appropriate number of cells is assigned automatically to the conductors. Specifically, a heuristic algorithm has been derived, which assigns cells by taking the relative length and width of the conductors into account. However, the number of cells per side should at least be three on all conductors for accurate solutions.

Appendix

The relative cell positions of interest can be narrowed down to the two general cases shown in Figs. 6 and 7. The coefficient [(6b)] for the relative cell location shown in Fig. 6 is

$$4\pi\epsilon p s_{ij} = \frac{1}{f_a f_b s_a s_b} \sum_{k=1}^{4} \sum_{m=1}^{4} (-1)^{i+j} \left[\frac{b_m^2 - C^2}{2} a_k \ln (a_k + \rho) + \frac{a_k^2 - C^2}{2} b_m \ln (b_m + \rho) - \frac{1}{6} (b_m^2 - 2C + a_k^2)\rho - b_m C a_k \tan^{-1} \frac{a_k b_m}{\rho C} \right] \quad (15)$$

where

$$\rho = (a_k^2 + b_m^2 + C^2)^{1/2}$$

and

$$a_1 = a_{ij} - \frac{f_a}{2} - \frac{s_a}{2}$$

$$a_2 = a_{ij} + \frac{f_a}{2} - \frac{s_a}{2}$$

$$a_3 = a_{ij} + \frac{f_a}{2} + \frac{s_a}{2}$$

TABLE I

COMPARISON OF TWO-DIMENSIONAL AND THREE-DIMENSIONAL SOLUTIONS

Capacitance Coefficient	Two Dimensional Solution Due to Weeks 5 matching points/side	Three dimensional Galerkin Solution Six cells along length	
		length/width = 1000	length/width = 10
$C_{11} = C_{33}$	0.286	0.297	0.325
$C_{12} = C_{23}$	- 0.0560	- 0.059	- 0.054
C_{22}	0.299	0.31	0.335
C_{13}	- 0.0083	- 0.0084	- 0.0077

The capacitances are in pF and are normalized to a length of 1 cm.

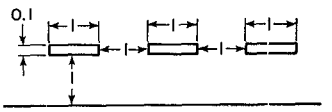

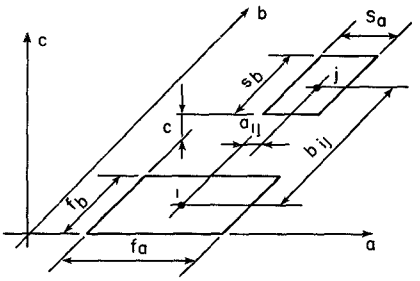

Fig. 6. Cells oriented in parallel.

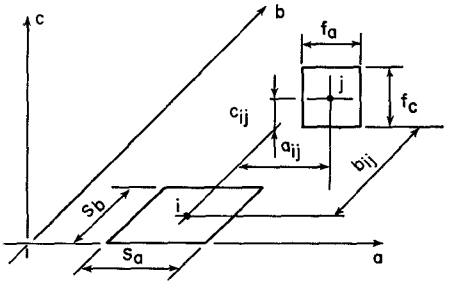

Fig. 7. Cells oriented perpendicular to each other.

$$a_4 = a_{ij} - \frac{f_a}{2} + \frac{s_a}{2}$$

$$b_1 = b_{ij} - \frac{f_b}{2} - \frac{s_b}{2}$$

$$b_2 = b_{ij} + \frac{f_b}{2} - \frac{s_b}{2}$$

$$b_3 = b_{ij} + \frac{f_b}{2} + \frac{s_b}{2}$$

$$b_4 = b_{ij} - \frac{f_b}{2} + \frac{s_b}{2}.$$

Similarly, for perpendicular cells, with the notation indicated in Fig. 7 the coefficient is

$$\begin{aligned} 4\pi\epsilon p s_{ij} = \frac{1}{f_a f_c s_a s_b} \sum_{k=1}^{4} \sum_{m=1}^{2} \sum_{l=1}^{2} (-1)^{l+m+k+1} \\ \cdot \left[\left(\frac{a_k^2}{2} - \frac{c_l^2}{6} \right) c_l \ln (b_m + \rho) \right. \\ + \left(\frac{a_k^2}{2} - \frac{b_m^2}{6} \right) b_m \ln (c_l + \rho) \\ + a_k b_m c_l \ln (a_k + \rho) - \frac{b_m c_l}{3} \rho \\ - \frac{a_k^3}{6} \tan^{-1} \left(\frac{b_m c_l}{a_k \rho} \right) \\ - \frac{b_m^2 a_k}{2} \tan^{-1} \left(\frac{a_k c_l}{b_m \rho} \right) \\ \left. - \frac{a_k c_l^2}{2} \tan^{-1} \left(\frac{a_k b_m}{c_l \rho} \right) \right] \end{aligned} \tag{16}$$

where ρ and a_k are defined as above and additionally

$$b_1 = b_{ij} + \frac{s_b}{2}$$

$$b_2 = b_{ij} - \frac{s_b}{2}$$

and where

$$c_1 = c_{ij} + \frac{f_c}{2}$$

$$c_2 = c_{ij} - \frac{f_c}{2}.$$

Both (15) and (16) are easily implemented in subroutine form in a computer program.

References

[1] K. G. Black and T. J. Higgins, "Rigorous determination of the parameters of microstrip transmission lines," *IRE Trans. Microwave Theory Tech.*, vol. MTT-3, pp. 93–113, Mar. 1955.

[2] A. Kessler, A. Vlcek, and O. Zinke, "Methoden zur Bestimmung von Kapazitäten unter besonderer Berücksichtigung der Teilflächenmethode," *Arch. Elek. Übertragung*, vol. 16, pp. 365–380, 1962.

[3] D. W. Kammler, "Calculation of characteristic admittances and coupling coefficients for strip transmission lines," *IEEE Trans. Microwave Theory Tech.*, vol. MTT-16, pp. 925–937, Nov. 1968.

[4] T. G. Bryant and J. A. Weiss, "Parameters of microstrip transmission lines and of coupled pairs of microstrip lines," *IEEE Trans. Microwave Theory Tech.*, vol. MTT-16, pp. 1021–1027, Dec. 1968.

[5] Y. M. Hill, N. O. Reckord, and D. R. Winner, "A general method for obtaining impedance and coupling characteristics of practical microstrip and triplate transmission line configurations," *IBM J. Res. Develop.*, vol. 13, pp. 314–322, May 1969.

[6] W. T. Weeks, "Calculation of coefficients of capacitance of multiconductor transmission lines in the presence of a dielectric interface," *IEEE Trans. Microwave Theory Tech.*, vol. MTT-18, pp. 35–43, Jan. 1970.

[7] P. Silvester, "TEM wave properties of microstrip transmission lines," *Proc. Inst. Elec. Eng.*, vol. 115, pp. 43–48, Jan. 1968.

[8] R. E. Collin, *Field Theory of Guided Waves*. New York: McGraw-Hill, 1960.

[9] J. C. Maxwell, Ed., *Electrical Researches of the Honourable Henry Cavendish*. Cambridge, England: Cambridge University Press, 1879.

[10] D. K. Reitan and T. J. Higgins, "Accurate determination of the capacitance of a thin rectangular plate," *AIEE Trans. Commun. Electron.*, vol. 75, pp. 761–766, Jan. 1957.

[11] S. Rush, A. H. Turner, and A. H. Cherin, "Computer solution for time-invariant electric fields," *J. Appl. Phys.*, vol. 37, pp. 2211–2217, May 1966.

[12] R. F. Harrington, *Field Computation by Moment Methods*. New York: Macmillan, 1968.

[13] J. A. Fuller and D. C. Chang, "On the numerical calculation of capacitance in the presence of edge boundaries," *Proc. IEEE* (Lett.), vol. 58, pp. 490–491, Mar. 1970.

[14] D. K. Reitan, "Accurate determination of the capacitance of rectangular parallel-plate capacitors," *J. Appl. Phys.*, vol. 30, pp. 172–176, Feb. 1959.

[15] D. K. Reitan and T. J. Higgins, "Calculation of the capacitance of a cube," *J. Appl. Phys.*, vol. 22, pp. 223–226, Feb. 1951.

[16] A. Farrar and A. T. Adams, "Computation of lumped microstrip capacitances by matrix methods—Rectangular sections and end effect," *IEEE Trans. Microwave Theory Tech.* (Corresp.), vol. MTT-19, pp. 495–497, May 1971.

[17] P. D. Patel, "Calculation of capacitance coefficients for a system of irregular finite conductors on a dielectric sheet," *IEEE Trans. Microwave Theory Tech.*, vol. MTT-19, pp. 862–869, Nov. 1971.

[18] P. Silvester and P. Benedek, "Equivalent capacitances of microstrip open circuits," *IEEE Trans. Microwave Theory Tech.*, vol. MTT-20, pp. 511–516, Aug. 1972.

[19] A. E. Ruehli, "Inductance calculations in a complex integrated circuit environment," *IBM J. Res. Develop.*, vol. 16, no. 5, Sept. 1972.

[20] ——, "Electrical analysis of interconnections in a solid-state circuit environment," *IEEE Int. Solid-State Circuit Conf. Dig.*, pp. 64–65, 1972.

[21] T. M. Apostol, *Mathematical Analysis, A Modern Approach to Advanced Calculus*. Reading, Mass.: Addison-Wesley, 1957.

[22] I. W. Kantorowitsch and W. I. Krylow, *Näherungsmethoden der höheren Analysis*. Berlin, Germany: Deutscher Verlag der Wissenschaften, 1956.

[23] D. S. Jones, *The Theory of Electromagnetism*. New York: Pergamon, 1964.

[24] A. E. Ruehli and D. M. Ellis, "Numerical calculation of magnetic fields in the vicinity of a magnetic body," *IBM J. Res. Develop.*, vol. 15, no. 6, Nov. 1971.

[25] E. Weber, *Electromagnetic Theory*. New York: Dover, 1965.

[26] G. Polya and G. Szegö, *Isoperimetric Inequalities in Mathematical Physics*. Princeton, N. J.: Princeton University Press, 1951.

[27] A. Ralston, *A First Course in Numerical Analysis*. New York: McGraw-Hill, 1965.

[28] J. R. Bunch and B. N. Parlett, "Direct methods for solving symmetric indefinite systems of linear equations," *SIAM J. Numer. Anal.*, vol. 8, Dec. 1971.

[29] C. Hoer and C. Love, "Exact inductance equations for rectangular conductors with applications to more complicated geometries," *J. Res. Nat. Bur. Stand.*, vol. 69C, pp. 127–137, Apr.–June 1965.

[30] C. Kittel, *Introduction to Solid State Physics*. New York: Wiley, 1968.

[31] S. Ramo, J. R. Whinnery, and T. V. Duzer, *Fields and Waves in Communication Electronics*. New York: Wiley, 1965.

The Variational Treatment of Thick Interacting Inductive Irises

TULLIO E. ROZZI

Abstract—**The problem of two thick interacting inductive irises in waveguide is treated with a variational approach.**

Using the appropriate Green's functions in the continuity equations of the transverse magnetic fields yields two coupled integral equations for the magnetic currents on the apertures. Solving one equation by Fourier expansion and introducing in the remaining equation, a variational expression for the driving-point admittance is obtained. This is treated with a Rayleigh–Ritz procedure and matrix methods, avoiding the explicit computation of field amplitudes.

The analysis is carried out in terms of an eigenmode expansion, as well as in terms of an expansion à la Schwinger on the aperture and the features of the two methods are contrasted.

In spite of its somewhat greater mathematical complexity, the latter generally provides a superior solution for a given order of the trial field.

In both cases the solutions are very accurate, uniformly convergent to their common limit value, and require manipulations with small-order matrices only. The agreement with the experiment is excellent.

Manuscript received May 30, 1972; revised September 21, 1972.

The author is with Philips Research Laboratories, Eindhoven, The Netherlands.

I. Introduction

THE PROBLEM of the inductive iris in waveguide, one of the geometrically simplest and most commonly used configurations, admits, nonetheless, no general analytical solution. On the other hand, the variational approach to this problem can be developed analytically to such an extent as to yield answers that can be as accurate as prescribed and, in the quasistatic limit, can even be cast in closed form.